# Overexpression of *Foxn1* attenuates age-associated thymic involution and prevents the expansion of peripheral CD4 memory T cells

Erin C. Zook,[1,2] Paulette A. Krishack,[1,2] Shubin Zhang,[3] Nancy J. Zeleznik-Le,[4] Anthony B. Firulli,[5] Pamela L. Witte,[1-3] and Phong T. Le[1-3]

[1]Cell Biology, Neurobiology and Anatomy Graduate Program, [2]Program for Immunology and Aging, [3]Department of Microbiology and Immunology, and [4]Department of Medicine, Division of Hematology/Oncology, Stritch School of Medicine, Loyola University Chicago, Maywood, IL; and [5]Riley Heart Research Center, Wells Center for Pediatric Research, Division of Pediatric Cardiology, Department of Anatomy, Indiana University Medical School, Indianapolis, IN

**The forkhead box n1 (Foxn1) transcription factor is essential for thymic organogenesis during embryonic development; however, a functional role of Foxn1 in the postnatal thymus is less well understood. We developed *Foxn1* transgenic mice (*Foxn1*Tg), in which overexpression of Foxn1 is driven by the human keratin-14 promoter. Expression of the *Foxn1* transgene increased the endogenous *Foxn1* levels. In aged mice, overexpression of *Foxn1* in the thymus attenuated the decline in thymocyte numbers, prevented the decline in frequency of early thymic progenitors, and generated a higher number of signal joint TCR excised circle. Histologic studies revealed that structural alterations associated with thymic involution were diminished in aged *Foxn1* Tg. Total numbers of EpCAM$^+$ MHC II$^+$ and MHC II$^{hi}$ thymic epithelial cells were higher in young and old *Foxn1*Tg and more EpCAM$^+$ MHC II$^{hi}$ TEC expressed Ki-67 in aged *Foxn1*Tg compared with WT. Furthermore, *Foxn1*Tg displayed a significant reduction in the expansion of splenic CD4$^+$ memory compartments and attenuated the decline in CD4$^+$ and CD8$^+$ naive compartments. Our data indicate that manipulation of *Foxn1* expression in the thymus ameliorates thymopoiesis in aged mice and offer a strategy to combat the age-associated decline in naive T-cell production and CD4 naive/memory ratios in the elderly. (*Blood*. 2011;118(22):5723-5731)**

## Introduction

It is well documented that aging negatively affects immune responses, leading to an increase in infection and mortality. Exactly how aging alters immune cell functions is not completely understood. Aging causes a decline in the production of naive T cells by the thymus; furthermore, intrinsic defects in mature T-cell functions, alterations in life span of naive T cells and in naive/memory T-cell ratios in the peripheral lymphoid tissues are documented.[1,2] It is thought that these age-associated changes culminate the decline in T-cell responses in the elderly. Understanding the cellular and molecular mechanisms that govern these changes would lead to novel approaches and strategies that can be used to ameliorate T-cell functional decline and promote thymic output of naive T cells in the elderly.

In postnatal life, the thymus is the primary organ that produces naive TCR$\alpha\beta$ T cells for the peripheral T-cell pool, albeit the production declines as early as 3 months of age.[3] Thymic epithelial cells (TECs) are the primary cell type of thymic stroma, critically responsible for thymopoiesis.[4] Functional maturation of TEC requires expression of the transcription factor forkhead box n1 (Foxn1); mutations in both mouse *Foxn1* and human *FOXN1* genes result in athymic and hairless conditions as seen in nude mice and patient with severe combined immunodeficiency syndrome.[5,6] We previously showed that the decline in the expression of *Foxn1* in thymic stroma correlates with the onset of reduction in thymocyte numbers and production of naive T cells as determined by the total number of signal joint TCR excised circle (sjTREC) in the thymus, suggesting that Foxn1 may play a role in age-associated thymic involution.[3] Subsequent work by others demonstrated a role of Foxn1 in the cross-talk between TEC and developing thymocytes, which is required for thymopoiesis.[7] Genetic approaches provide data to strengthen a supporting role of Foxn1 in thymopoiesis in the postnatal thymus, demonstrating that induced deletion of *Foxn1* or reduced expression leads to premature thymic involution, whereas the presence of Foxn1$^+$ TEC is essential for maintaining thymopoiesis.[8-11] Hence, preventing the decline in *Foxn1* expression in the context of aging could rescue age-associated thymic involution.

We used a transgenic (Tg) approach to generate *Foxn1* overexpressing mice in which expression of *Foxn1* is driven by the human keratin-14 (K14) promoter. We report here that thymic involution is attenuated as seen by the delay in the decline in thymopoiesis in aged *Foxn1*Tg compared with wild-type mice (WT). The attenuation in thymic involution reflects the intact thymic architecture, higher number of EpCAM$^+$ cells, and higher levels of the early T lineage progenitors (ETPs) found in aged *Foxn1*Tg mice. In addition, the attenuation of thymic involution abated the decline in CD4$^+$ and CD8$^+$ naive compartments and prevented the age-associated expansion of the peripheral CD4$^+$ memory T cell. Lastly, the finding that expression of *Foxn1* can be up-regulated in the aged thymus suggests that strategies to reverse the decline in *Foxn1* expression with advancing age can be used to ameliorate thymopoiesis and potentially improve immune responses in the elderly.

Submitted March 11, 2011; accepted August 5, 2011. Prepublished online as *Blood* First Edition paper, September 9, 2011; DOI 10.1182/blood-2011-03-342097.

The online version of this article contains a data supplement.

The publication costs of this article were defrayed in part by page charge payment. Therefore, and solely to indicate this fact, this article is hereby marked "advertisement" in accordance with 18 USC section 1734.

**Table 1. Primer sequences**

| Gene | Forward | Reverse | Reference |
|---|---|---|---|
| *Foxn1*$^{endo}$ | GACCTTGGGACTGACCTGGAT | TGCCTGTTTCTGCCAGACAA | NM_008238.1 |
| *Foxn1* $^{Tg}$ | CTTGAGCTATGCCCAACATCAG | GCTGTATTGATTGCCAGGAGG | |
| *Gapdh* | GTGAGGCCGGTGCTGAGTAT | CATCCTGCACCACCAACTGCTTAGCC | M32599 |
| *φJα1* | CAGGGAAGATGGGCCTCTCT | GAAGGCATAAACCGACACGAA | AE000663 |
| *TCRDβ1* | GACACCCAGCGCCAAGAA | CACCGTGGCCCCCTGT | AE000664 |
| *TCRDβ2* | TCCCAAGGACATCTCCAAGCT | GGCTGAGAGTTGGTGTTTTTTTG | AE000665 |
| *TCRCβ2* | AGAGGATCTGAGAAATGTGACTCCA | GCCAGAAGGTAGCAGAGACCCT | NT_039341.7 |

Primer Express software was used to generate the selected sequences.

## Methods

### *Foxn1*Tg

The mouse *Foxn1* cDNA fragment (2.1 kb) from nucleotide positions 78 to 2255 (NM_008238.1) was cloned into the BamH1 site of the human K14 promoter expressing cassette pG3ZK14 (K14-Foxn1; Dr Elaine Fuchs, Rockefeller University, New York, NY). The K14-Foxn1expression construct was sequenced to confirm the correct orientation and its open reading frame. The 5.5-kb NarI-VspI fragment of the K14-Foxn1 construct was used to generate Tg mice on the B6D2F1 background using standard protocol. Tg founders (lines 60 and 5) were first identified by southern blot analysis and subsequently by PCR analysis of tail genomic DNA using the Extract-N-AMP tissue PCR kit (Sigma-Aldrich). Tg founders were identified using primers specific for rabbit β-globin intron-Foxn1 (5′-end) and Foxn1-human K14 polyA (3′-end) junctions. Founders were backcrossed to the B6 background for 13 generations. Transgene copy numbers were determined by quantitative PCR using primers specific for exon 3 of *Foxn1* gene. C57Bl/6 mice were purchased from Harlan or NIA and served as controls. All animal work was performed according to protocols approved by Loyola University Stritch School of Medicine Institutional Animal Care and Use Committee.

### Quantification of *Foxn1* mRNA levels in thymic stroma

Thymic stroma samples were obtained from young and old WT and *Foxn1*Tg by gentle teasing and repeatedly washing to remove thymocytes; total RNA was isolated using Trizol reagent (Sigma-Aldrich) according to the manufacturer's protocol. Isolated RNA was then treated with DNase using Ambion DNA-free kit and 0.5 to 2 μg of RNA was used for cDNA synthesis using the Invitrogen's SuperScript II synthesis kit. Quantitative RT-PCR was performed on an Applied Biosystems 7300 as previously described.[3] To differentiate the expression levels of the endogenous and transgene *Foxn1* in *Foxn1* Tg mice, 2 sets of primer were designed. The first primer set recognize both the endogenous (Foxn1$^{Endo}$) and the transgene (Foxn1$^{Tg}$) *Foxn1* transcripts; this primers set was used to determine the total levels of *Foxn1* (Foxn1$^{Total}$). The second primer set only detects the *Foxn1* transgene (Foxn1$^{Tg}$). The levels of endogenous *Foxn1* mRNA were then calculated by subtracting Tg *Foxn1* levels from total *Foxn1* levels (Foxn1$^{Endo}$ = Foxn1$^{Total}$ − Foxn1$^{Tg}$). Primer sequences are presented in Table 1. Samples were normalized to the housekeeping gene *Gapdh*. Levels of *Foxn1* expression were extrapolated from a standard curve constructed with 5 known concentrations ranging from 10 copies/μL to 100 000 copies/μL. Levels of *Foxn1* were expressed as copy numbers/μg RNA.

### Immunofluorescence and H&E staining

Acetone-fixed frozen thymi sections (4-5 μm) in OCT media were used for immunofluorescent studies. Anti-Foxn1 antibody was raised in rabbits against a Foxn1 peptide (amino acid 303-324, exon 6). Sections were blocked with Super Block (ScyTek) and then incubated with either rabbit anti–mouse Foxn1 (IgG, 100-150 μg/mL), rabbit anti–mouse keratin 5 (0.1 μg/mL, Covance), rat anti–mouse keratin 8 (0.221 μg/mL, DSHB), rabbit IgG (Invitrogen), or rat IgG (BD Biosciences). Sections were then washed and incubated with goat anti–rabbit IgG-FITC, goat anti–rabbit IgG- AF488, or goat anti–rat IgG-AF546 F(ab)$_2$′ (10 μg/mL; Invitrogen). Sections were analyzed using a Zeiss confocal LSM 510 microscope. For H&E staining, thymic tissues were fixed in formalin and then embedded in paraffin.

### Flow cytometry

One million ($1 \times 10^6$) thymocytes from WT and *Foxn1*Tg were blocked with an anti-Fc receptor antibody CD16/32 and stained with a cocktail containing FITC-conjugated antibodies specific for lineage-positive markers CD3, CD8, B220, CD49b, CD11b, Gr-1, and Ter119. Thymocytes were then stained with anti–mouse CD117, CD25, CD44, and CD127. ETPs were identified as lin$^-$ CD117$^+$ CD44$^{hi}$ CD25$^-$ CD127$^-$, and the frequency of ETP was expressed as number of ETP/100 000 thymocytes. Thymic stromal cells were stained with CD45, EpCAM, MHC II, and Ly51, followed by fixation and permeabilization for Ki67 staining. Medullary thymic epithelial cells (mTECs) were identified as CD45$^-$ EpCAM$^+$ Ly51$^-$ that were either MHC II$^+$ or MHC II$^{hi}$. Total number of ETP and mTECs was calculated from the frequencies and total number of isolated thymocytes or thymic stromal cells. Flow cytometric data were analyzed using FlowJo Version 7.5.5 (TreeStar). Antibody information is summarized in Table 2.

### Isolation of thymic stromal cells

Thymi were removed, injected with 0.05 mg/mL liberase (Roche Diagnostics), and incubated at room temperature for 8 minutes before dispersing by gentle teasing and pipetting. Digestion continued at 37°C for 35 minutes with the addition of DNAse (0.2 mg/mL), and thymic stromal cells were released mechanically and enriched using a 50% to 25% step Percoll (Sigma-Aldrich) gradient (unpublished protocol from T. D. Logan and A. Bhandoola, University of Pennsylvania).

### Quantification of sjTREC, TCR-Dβ1, and TCR-Dβ2 germline levels

Genomic DNA from $1 \times 10^6$ thymocytes was isolated using DNAzol (Invitrogen) according to the manufacturer's protocol. The sjTREC levels

**Table 2. Antibodies, specific clones, and fluorochromes for flow cytometry**

| Antibody | Clone | Fluorochrome | Source |
|---|---|---|---|
| CD16/32 | 2.4G2 | Purified | eBioscience |
| CD3 | 145–2c11 | FITC | eBioscience |
| CD8 | 53–6.7 | FITC | eBioscience |
| B220 | RA3–6B2 | FITC | eBioscience |
| CD49b | DX5 | FITC | eBioscience |
| CD11b | MI/70 | FITC | eBioscience |
| Gr-1 | RB6–8C5 | FITC | eBioscience |
| Ter119 | Ter119 | FITC | eBioscience |
| CD117 | D7 | PE | eBioscience |
| CD44 | IM7 | AF750 | eBioscience |
| CD25 | PC61.5 | APC | eBioscience |
| CD127 | A7R34 | PECy7 | eBioscience |
| CD45 | 30-F11 | Percp | BD Biosciences PharMingen |
| MHC II | M5/114.15.2 | AF780 | eBioscience |
| EpCAM | G8.8 | APC | eBioscience |
| Ly51 | 6C3/BP-1 | PE | eBioscience |
| Ki67 | B56 | AF488 | eBioscience |

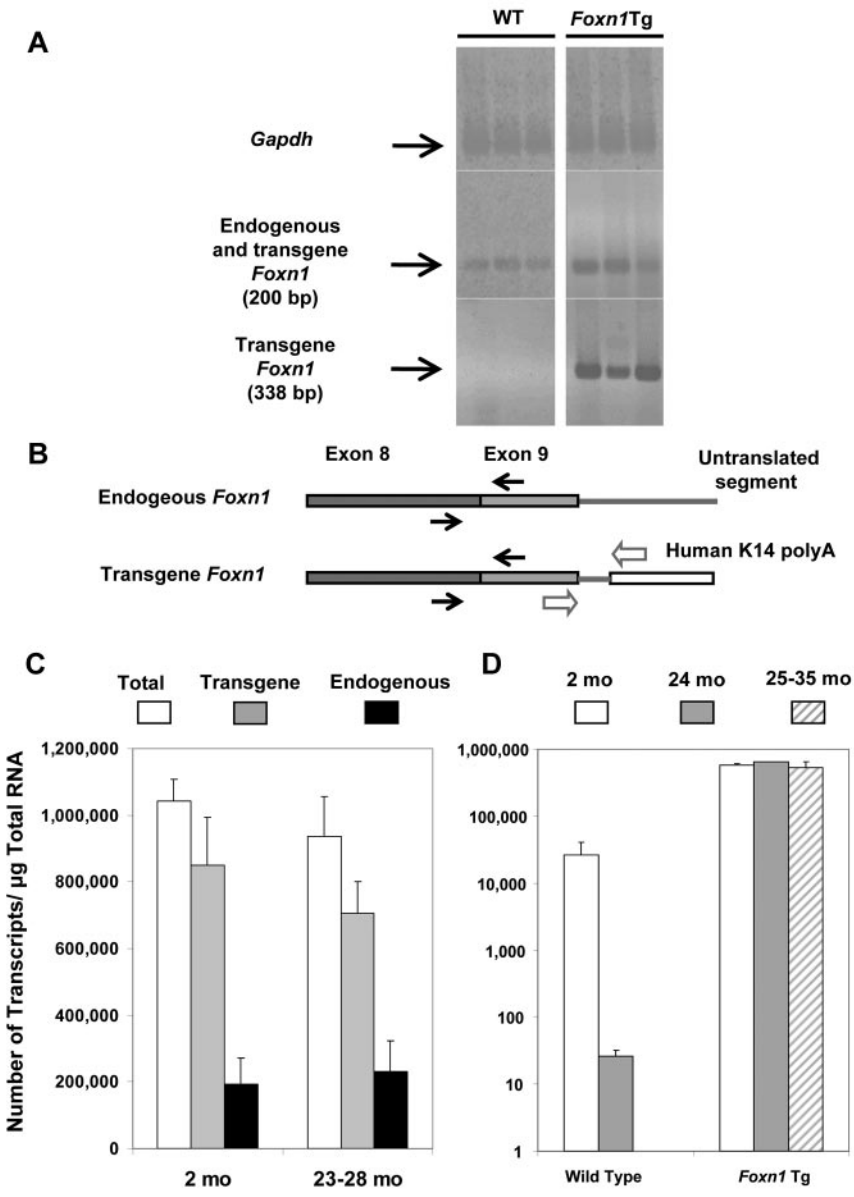


**Figure 1. Quantification of endogenous and Tg *Foxn1* expression by quantitative RT-PCR.** (A) RT-PCR shows specificity of primers that detect both the endogenous and transgene *Foxn1* and primers that only detect transgene *Foxn1* transcripts. Each lane represents results from a WT or *Foxn1*Tg mouse (line 60). (B) Diagram showing the relative positions of the forward and reverse primers that detect either both endogenous and transgene (arrows) or only Tg (arrow outlines) *Foxn1* transcripts. (C) Expression of the endogenous and transgene *Foxn1* in 2-month-old (n = 3) and 23- to 28-month-old (n = 3) Tg line (line 60). The numbers of transcripts per microgram of total RNA were calculated from a standard curve after normalization with the mouse housekeeping gene *Gapdh*; each sample was performed in triplicates. The endogenous *Foxn1* levels were determined by subtracting the total *Foxn1* (endogenous plus transgene) from that of the transgene. White bars represent the total *Foxn1* levels; gray bars, Tg *Foxn1*; and black bars, endogenous *Foxn1*. Errors bars represent SD. (D) Expression of total *Foxn1* in WT (n = 2 at 2 months; n = 3 at 24 months) and in the 2 *Foxn1*Tg lines (line 60: n = 3 at 2 months and n = 3 at 24 months; line 5: n = 4 at 25-35 months). WT: white bar represents 2 months of age; and gray bar, 24 months of age. *Foxn1* Tg: white bar represents 2 months of age; gray bar, 24 months of age (line 60); crossed bars represent 25 to 35 months of age (line 5). y-axis is in logarithmic scale. Errors bars represent SD.

were determined by quantitative PCR using 80 ng of genomic DNA as previously described.[3] The same amount of DNA was used to determine the levels of germline TCR-Dβ1 and Dβ2; primers specific for Dβ1 and Dβ2 were designed such that only the germline configurations of the 2 genes were detected while any DJ rearrangements result in the loss of the sequences specific for the reverse primers. Standard curves consisting of the following concentrations were used to calculate copy numbers of sjTREC, TCR-Dβ1, and TCR-Dβ2: 100 000, 10 000, 1000, 100, and 10 copies/μL. The levels of TCRCβ2 (exon 1) were used to normalize all samples. Primer sequences were presented in Table 1.

## Results

### Expression of *Foxn1* in the thymus of *Foxn1*Tg mice

We determined that the homozygous *Foxn1*Tg line 5 has 10 to 12 copies and the *Foxn1*Tg line 60 has 4 or 5 copies of the transgene (data not shown). To determine the contribution of the endogenous and transgene *Foxn1* expression in the 2 Tg lines, we designed primers specific only for the transgene *Foxn1* and common primers that amplify both the transgene and endogenous *Foxn1* transcripts. Figure 1A shows that the transgene-specific primers only detected *Foxn1* mRNA in thymic stroma from *Foxn1*Tg whereas the common primers detected *Foxn1* mRNA in both WT and *Foxn1*Tg thymic stroma. Figure 1B shows the relative positions of the 2 sets of primers within the endogenous and transgene *Foxn1* transcripts. Expression of the transgene *Foxn1* for the 2-month-old Tg line 60 was approximately 4-fold higher than the endogenous *Foxn1*; both endogenous and transgene levels were not changed with age (Figure 1C). In contrast, thymi from C57Bl/6 WT mice showed a 1000-fold reduction in expression of *Foxn1* with age (Figure 1D), similar to our previous observations in BALB/c mice.[3] The overall levels of expression of *Foxn1* in the *Foxn1*Tg mice were 20-fold higher compared with that in young C57Bl/6 mice. Furthermore, the levels of *Foxn1* expression in both Tg lines were similar and not reduced with age (Figure 1D). Interestingly, expression of endogenous *Foxn1* in the 2-month-old *Foxn1*Tg is 7.2-fold higher than that found in the young WT mice (192 303 vs 26 628), suggesting that overexpression of the transgene induces expression of the endogenous *Foxn1* (Figure 1C-D).

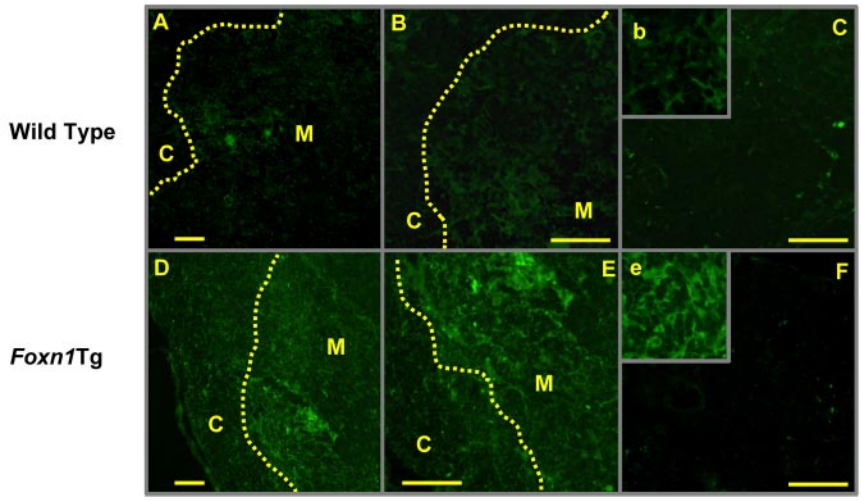


**Figure 2. Detection of Foxn1-expressing stroma cells in the thymus of WT and *Foxn1* Tg mice (2-3 months) by immunofluorescent staining.** Frozen sections (4-5 μm) were fixed in acetone and stained with a rabbit anti-Foxn1 antibody (IgG fraction) or purified rabbit IgG control antibody, followed by incubation with FITC-conjugated goat anti–rabbit IgG $F(ab)_2'$. (A-B,D-E) Stained with anti-Foxn1 antibody. (C,F) Stained with purified rabbit IgG antibody. Slides were studied using Zeiss LSM 510 confocal microcopy (A,C-D,F, original magnification 25×/0.8 W; B,E, original magnification 40×/1.2 W). Insets b and e represent an enlargement of the medulla regions in panels B and E, respectively. Scale bars represent 50 μm.

### Overexpression of *Foxn1* and thymopoiesis in young mice

We next determined whether high levels of expression of *Foxn1* affected thymic architecture in the young Tg mice. Using a rabbit polyclonal antibody raised against Foxn1 peptide and immunofluorescent staining, we found that expression of *Foxn1* in the WT thymus (2-3 months) was prominent in the thymic medulla with scattered $Foxn1^+$ cells in the thymic cortex (Figure 2A-B inset b). Expression of *Foxn1* in Tg mice was also detected in thymic medulla as well as cortex with a similar expression pattern; however, staining appeared more prominent compared with that in the WT thymus (Figure 2A-B,D-E insets b,e). Thus, the enhanced intensity staining of Foxn1 reflected the increase in the expression at the mRNA levels of both the transgene and endogenous *Foxn1*. Functionally, the overexpression of *Foxn1* did not affect the development of thymocytes as determined by the normal distribution of CD4, CD8 double-negative, double-positive, and single CD4- or CD8-positive subsets compared with that found in WT mice (supplemental Figure 1, available on the *Blood* Web site; see the Supplemental Materials link at the top of the online article).

### Overexpression of *Foxn1* attenuates age-associated decline in thymopoiesis as measured by thymocyte numbers and ETP frequencies

Because overexpression of *Foxn1* does not affect thymopoiesis in young mice, we determined whether age-associated decline in thymopoiesis is affected in aged *Foxn1*Tg. As shown in Figure 3A, aged *Foxn1* Tg (13 months) had relatively larger thymi, few foci of adipose tissue, and higher number of total thymocytes compared with age-matched WT. We determined the frequencies of sjTREC/$10^5$ thymocytes and total number of sjTREC as readout of naive T-cell output in the thymi of *Foxn1*Tg versus WT mice at 12 to 15 months of age. The thymi from *Foxn1*Tg averaged 1.7-fold higher in frequency of sjTREC/$10^5$ cells and 2.8-fold higher in the total number of sjTREC/thymus (Figure 3B-C, $P = .019$; $P = .004$). Conversely, we observed significantly lower copy numbers of the germline TCR-Dβ1 in aged *Foxn1*Tg compared with the age-matched WT ($P = .044$), indicating that a higher number of the TCR-Dβ loci are rearranged in thymocytes from *Foxn1*Tg (Figure 3D). Although we detected a similar trend for the TCR-Dβ2 locus, the differences were not quite significant ($P = .063$).

To further demonstrate that overexpression of *Foxn1* improves thymopoiesis with age, we determined changes in the number of thymocytes in WT and *Foxn1*Tg that were > 2 years old. Although the number of thymocytes in WT declined rapidly during middle age (by 16-19 months) and then showed a more protracted reduction in the 20- to 26-month age group, the reduction in the number of thymocytes in *Foxn1*Tg progressed with a much reduced magnitude (Figure 4A). Compared with the 3-month-old mice, there was a 3.7-fold reduction in the number of thymocytes in WT by 16 to 19 months of age, but the number of thymocytes in *Foxn1*Tg of the same age group was reduced only by 1.4-fold (Figure 4A). By 20 to 26 months of age, we observed a 5.3-fold reduction compared with 3 months in WT but only a 3-fold reduction in *Foxn1*Tg (Figure 4A). Furthermore, we analyzed a group of 6 *Foxn1*Tg killed at 29 to 32 months of age and determined that the number of thymocytes in these *Foxn1*Tg were not different from those of the WT 20 to 26 months of age ($14.2 \times 10^6 \pm 13.3 \times 10^6$ WT vs $18.8 \times 10^6 \pm 11.3 \times 10^6$ Tg; $P = .83$, data not shown). Thus, our data strongly indicate that overexpression of *Foxn1* in the thymus attenuates the age-associated decline in thymopoiesis in *Foxn1*Tg. Based on the total number of thymocytes, we estimated that the decline in thymopoiesis in *Foxn1*Tg lags behind WT approximately 6 to 8 months.

ETP frequencies and total number have been shown to decline with age.[12] To begin understanding the cellular mechanism by which thymic involution is attenuated in aged *Foxn1*Tg, we determined whether the ETP population is affected with age in WT and *Foxn1*Tg. As previously shown with advanced age, the frequency of ETP/$10^5$ cells and the total number of ETPs were significantly reduced in WT[12] (Figure 4B-C). However, the ETP frequencies were not affected, and the decline in total ETP number was attenuated with age in the *Foxn1*Tg. ETP frequencies were not only significantly higher in the aged *Foxn1*Tg compared with those in aged WT ($P = .038$), but the levels were also not significantly different from those found in young WT and *Foxn1*Tg ($P = .233$, $P = .534$, Figure 4B); the total number of ETPs in old *Foxn1*Tg mice was 2.7-fold higher than in aged WT ($P = .047$, Figure 4C).

### Overexpression of *Foxn1* prevents age-associated changes in cortical and medullary thymic architecture

A hallmark of aged-associated thymic involution is the reduction in size and the accumulation of adipose tissue in thymic parenchymal tissue, resulting in a fatty appearance of the thymus gland and a reduction in thymocyte numbers.[13] As shown in Figure 3, at a gross level of observation, thymi from 2 *Foxn1*Tg (13 months) displayed a homogeneous opacity with no obvious appearance of adipose

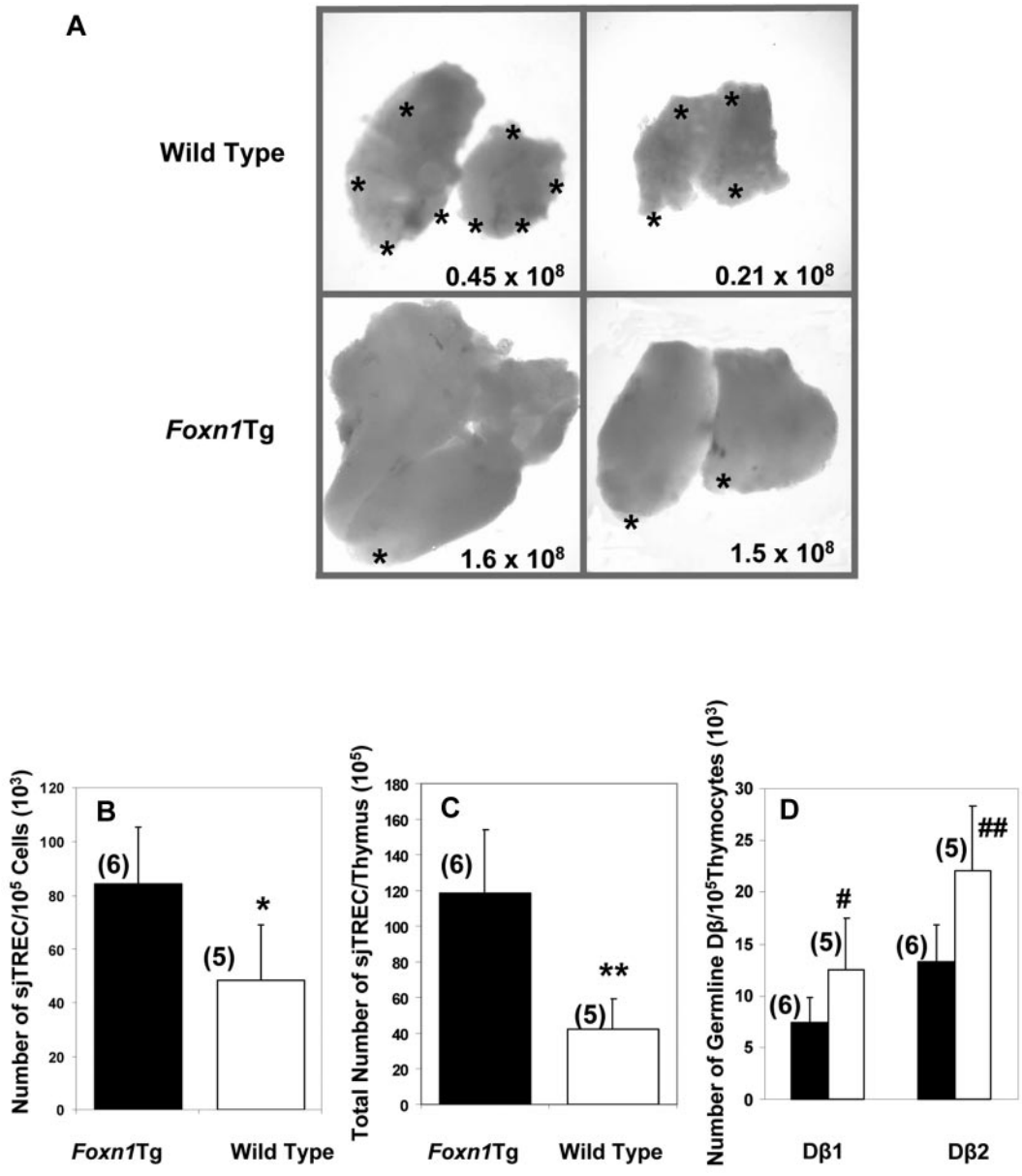


**Figure 3. Gross morphology and TCR rearrangement in aged WT and *Foxn1*Tg.** (A) Gross morphology of thymi from 2 WT (top) and 2 *Foxn1*Tg (line 60) mice 13 months of age (bottom). The numbers denote total number of thymocytes obtained from each thymus. *Translucent/fatty areas of the thymus. (B-C) Rearrangement of TCR-α chain was measured as the number of sjTREC/$10^5$ thymocytes (B), and total number of sjTREC/thymus (C) in old (12-15 months of age) *Foxn1*Tg (line 60 and line 5) and WT mice. (D) D-J rearrangement of TCR-β chain was determined by the number of germline copies of Dβ1 and Dβ2; black bars represent *Foxn1* Tg; and white bars, WT mice. Quantitative PCR was used for both assays; each sample was performed in triplicates. Values in parentheses indicate the numbers of mice in each group. *P* values from comparison between WT and *Foxn1*Tg mice as determined by *t* test are as follows: **P* = .019; ***P* = .004; #*P* = .040; ##*P* = .063.

tissue, which appears as translucent areas present in thymi from age-matched WT. A histologic study was performed to determine whether changes seen in an involuted thymi from WT were also observed in *Foxn1*Tg. Figure 5A-B shows a fatty thymus of a 26-month-old WT with altered thymic architecture as determined by the loss of cortical-medullary demarcation. As a comparison, a thymus from a much older *Foxn1*Tg (line 60, 31 months) showed little adipose tissue deposition and a well-defined cortical-medullary demarcation (Figure 5C-F).

We next analyzed the expression patterns and the intensities of keratin 8 and keratin 5, which demarcate thymic cortex and medulla, respectively. The intensity of keratin 8 staining (red) was less in 26-month thymi compared with that determined in 2-month WT (Figure 6B,C vs A). Compared with WT, *Foxn1* Tg (31 months) displayed intense keratin 8 staining in the thymic cortex, showing few areas that were devoid of staining (Figure 6E-F). We also observed a disorganized medullary region as visualized by filamentous staining pattern of keratin 5 (green) as well as the collapse of discreet regions of keratin 5-positive cells into a fused medullary region in old WT mice (Figure 6B-C). In contrast, the patterns of keratin 5 staining in *Foxn1*Tg displayed a more discrete and distinct medullary foci similar to that found in young mice (Figure 6D-F). Thus, overexpression of *Foxn1* dampened the age-associated alterations in thymic architecture.

### Overexpression of *Foxn1* increases the number of EpCAM$^+$ cells and maintains a higher number of EpCAM$^+$ with age

It has been shown that aging causes a reduction in the CD45$^-$ thymic stroma fraction, mainly because of a reduction in the highly

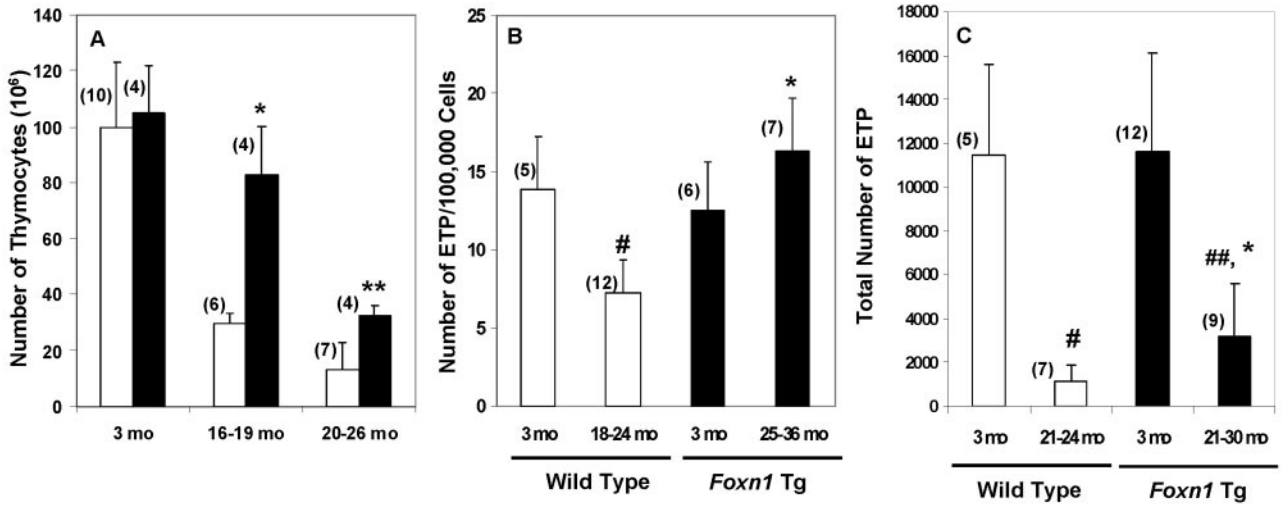


**Figure 4. Thymocyte and ETP numbers in WT and *Foxn1*Tg.** (A) Thymocyte numbers in 3-month-old, 16- to 19-month-old, and 20- to 26-month-old WT (white bars) and *Foxn1*Tg (line 60; black bars). *P* values from comparison between WT and *Foxn1*Tg as determined by *t* test or Mann-Whitney are as follows: $*P = .043$ and $**P = .012$, respectively. (B) Frequencies of ETP in WT (white bars) and *Foxn1*Tg (black bars). ETP are defined as $Lin^- CD117^+ CD44^{hi} CD25^- C127^-$. WT 3-month-old versus WT 18- to 24-month-old: $\#P = .009$; *Foxn1*Tg 25- to 36-month-old versus WT 18- to 24-month-old: $*P = .038$ (*P* values from *t* test). (C) Total number of ETP in WT (white bars) and *Foxn1*Tg (black bars) mice. WT 3-month-old versus 21- to 24-month-old: $\#P = .003$; *Foxn1*Tg 3-month-old versus 21- to 30-month-old: $\#\#P < .001$; *Foxn1*Tg 21- to 30-month-old versus WT 21- to 24-month-old: $*P = .047$ (*P* values from *t* test). Error bars represent SD. Values in parentheses represent the number of mice in each group. Data were from line 5 and line 60.

proliferating MHC $II^{hi}$ TEC subset.[14] Reduction of *Foxn1* expression is correlated with a reduction in mTECs, specifically with the loss of MHC $II^{hi}$ $UEA^+$ mTECs, which express high levels of *Foxn1*.[9,10] We found that the total number of MHC $II^+$ $EpCAM^+$ $Ly51^-$ TECs was 2.5-fold higher in 3-month-old *Foxn1*Tg compared with WT ($P = .003$, Table 3). Because it has been shown that the MHC $II^{hi}$ TEC is responsible for the size of the medullary compartment, we determined the number of MHC $II^{hi}$ $EpCAM^+$ $Ly51^-$ TECs and found that it was 5-fold higher in *Foxn1*Tg ($P < .001$, Table 3). Aging resulted in reduction of both MHC $II^+$ and MHC $II^{hi}$ $EpCAM^+$ subsets; however, their numbers remained significantly higher in *Foxn1*Tg compared with WT ($P = .023$, $P = .040$, Table 3). We also found that the percentages of $Ki67^+$ were higher (2-fold) in aged *Foxn1*Tg compared with aged WT ($P = .017$, Table 3). However, cortical TEC numbers were equivalent in aged *Foxn1*Tg and WT (data not shown). Flow cytometric profiles of isolated TECs are presented in supplemental Figure 2.

### Attenuation of age-associated thymopoiesis affects the peripheral naive and memory T-cell compartment

It is well established that the decline in the production and egress of naive T cells from the thymus with age results in the contraction of the peripheral CD4 and CD8 naive T-cell compartments and a concomitant expansion of the memory compartments. Therefore, we determined whether attenuation of thymic involution in aged *Foxn1*Tg affected the peripheral memory pools. Splenic naive and memory T cells were defined as $CD3^+$ T cells that were $CD44^+$ or $CD44^{hi}$, respectively. As expected, the total number of $CD3^+$ T cells in the spleen was not significantly changed with age in WT or *Foxn1*Tg (Figure 7). However, the $CD4^+$ naive compartment in WT showed a significant decline from 57% at 2 to 3 months to 30% at 20 to 25 months and to 11% at 28 to 35 months; similarly, the $CD8^+$ naive compartment declined from 14% to 6% and to 3% (Figure 7 top panels). Concurrently, the $CD4^+$ memory compartment in WT increased from 21% to 44% and to 47%, and the $CD8^+$ memory compartment increased from 9% to 20% and to 39% (Figure 7 top panels). In contrast, the decline in naive $CD4^+$ and $CD8^+$ in the $CD3^+$ pool was less severe in *Foxn1*Tg compared with WT; we determined only a 2-fold reduction (28-35 months vs 2-3 months) for naive $CD4^+$ and 1.4-fold for naive $CD8^+$ in *Foxn1*Tg compared with a 5.2-fold and 4.7-fold decline in WT, respectively (Figure 7). Within the memory compartments, we detected a similar fold increase in the expansion of $CD8^+$ memory compartment in WT and *Foxn1*Tg (3.7-fold in Tg and 4.3-fold in WT). Interestingly, although there was a 2.2-fold increase in the expansion of memory $CD4^+$ in WT, no significant expansion in the $CD4^+$ memory compartment was detected in *Foxn1*Tg (Figure 7). Furthermore, the fractions of $CD4^+$ and $CD8^+$ naive cells were significantly higher in the *Foxn1*Tg at 28 to 35 months compared with WT within the same age group ($P = .038$ for CD4 and $P = .058$ for CD8, Figure 7). Conversely, the fraction of $CD4^+$ memory compartment in the *Foxn1*Tg mice was significantly less than that found in WT mice (26% vs 47%, $P = .0019$).

## Discussion

We have previously shown that expression of Foxn1 in the thymus declines as early as 3 months and occurs concurrently with the onset of a reduction in the total number of thymocytes and total sjTREC/thymus.[3] To investigate functional roles of Foxn1 in thymopoiesis in the postnatal thymus, we generated *Foxn1*Tg in which expression of *Foxn1* is driven by the human K14 promoter. We selected K14 promoter because K14 is expressed in epithelial stem cells and in thymic epithelial cell precursors.[15,16] The 2 Tg lines that we have generated have low copy numbers of the transgene (4 or 5 and 10-12 copies); however, both express *Foxn1* at a level 20-fold higher than in the C57Bl/6 WT mice. More importantly, *Foxn1* expression in both Tg lines was not reduced with age.

How expression of *Foxn1* is regulated, particularly with age, is not known. Although a 3-dimensional organization of TEC is required for maintenance of *Foxn1* expression, upstream signals/factors that regulate expression of *Foxn1* during thymic organogenesis and in postnatal thymus remain elusive.[17,18] It has been suggested that members of the Wnt glycoprotein family can

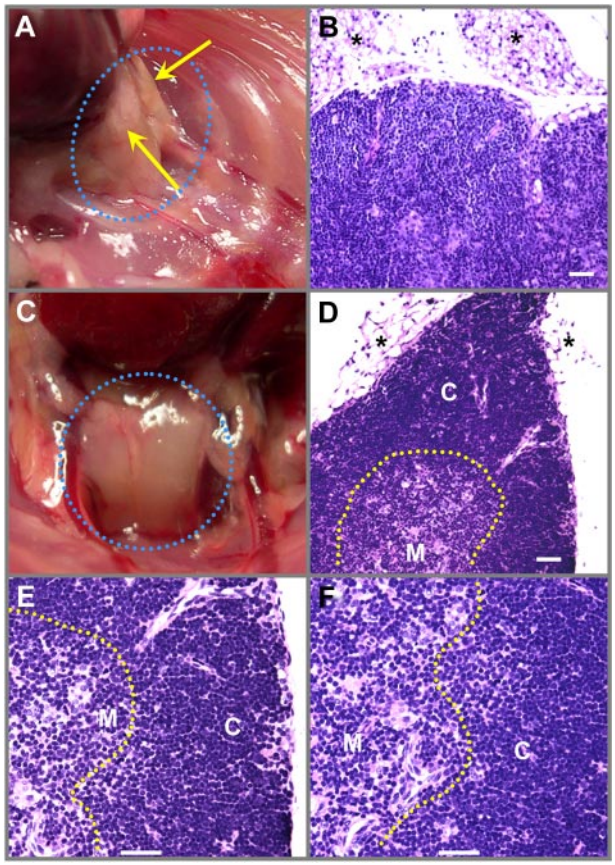


**Figure 5. Changes in gross thymic morphology and histology of old WT and *Foxn1* Tg mice (line 60).** (A) Gross thymic morphology of a 26-month-old WT mouse with adipose tissue present (arrows). (B) H&E staining of the same thymus shows the loss of cortical-medulla demarcation and the abundance of adipose tissue (*). (C) Gross thymic morphology of a 31-month-old *Foxn1*Tg mouse with intact parenchymal tissue with little adipose tissue deposition. (D-F) H&E staining of the same thymus shows a clear cortical-medulla demarcation and little adipose tissue deposition. Images were acquired with a Leitz Diaplan microscope with a 25×/0.6 W (B-D) and 50×/1.0 W equipped with Religa 2000R camera and QImaging Pro software (Version 6.0). Scale bars represent 50 μm.

regulate expression of *Foxn1* in vitro.[19] In hair follicles, BMP4 has been shown to up-regulate *Foxn1* expression.[20] BMP4 has also been shown to localize to cells in the ventral region of the third pharyngeal endoderm that later express *Foxn1* and are responsible for thymic organogenesis.[21] Direct evidence that links BMP4 and *Foxn1* expression in the aged thymus, however, is lacking.

The *Foxn1*Tg provide a unique in vivo mouse model to test whether overexpressing *Foxn1* transgene affects expression of endogenous *Foxn1*. We discovered that overexpression of the transgene *Foxn1* significantly increased expression of the endogenous gene, suggesting that Foxn1 acts in cis to regulate its own expression. Indeed, we found that stable mouse OP9 and human TEC cell lines that overexpress the mouse and human *FOXN1* (OP9-Foxn1, TE84-FOXN1) induced expression of the endogenous mouse *Foxn1* and human *FOXN1* genes (data not shown). Thus, the in vitro observations in the 2 cell lines recapitulate findings obtained from the in vivo *Foxn1*Tg model. Our finding that expression of *Foxn1* is self-regulated fulfills the previous suggestive notion that Foxn1 functions in a cell-autonomous fashion and underscores the finding that TECs that express a high level of Foxn1 are more sensitive to Foxn1 levels.[10,18] Furthermore, the same induced levels of the endogenous *Foxn1* in young and old mice suggest that down-regulation of *Foxn1* with age is totally reversible and can be manipulated to reverse expression of *Foxn1* in the aged thymus.

Because expression of *Foxn1* in our *Foxn1*Tg is not reduced with age, we could directly determine whether maintaining expression of *Foxn1* at higher than the normal physiologic level would have an effect on thymopoiesis in young and old mice. In the WT thymus, we found that Foxn1 is predominantly expressed in the medulla; however, scattered Foxn1$^+$ TECs were also found in the cortex. This pattern of Foxn1 expression is similar to previous findings reported by others in which Foxn1$^+$ cells were tracked by the expression of *Gfp* driven by the Foxn1 promoter.[22] The predominantly medullary pattern of expression is similar in the *Foxn1*Tg. The intensity of the staining appears stronger in the Tg thymus, which corroborates the high expression of *Foxn1* at the mRNA level. The pattern of expression also correlates with K14 promoter activity. K14 protein forms a heterodimer complex with keratin 5, which is predominantly expressed in mTECs and in a minor population of cortical TECs.[23,24] Thus, K14-driven expression of *Foxn1* in the Tg thymus closely emulates the expression of the endogenous *Foxn1* and does not alter thymopoiesis as supported by the normal distribution of CD4, CD8 double-positive, CD4$^+$ and CD8$^+$ single-positive cells and CD4, CD8, CD3 triple-negative. We did observe, however, a significantly higher fraction of the single CD3$^+$ CD8α$^+$ T cells ($73.3 \pm 0.5$ vs $59 \pm 6.2$, $P = .011$) and concomitantly a reduced level of CD3$^-$ CD8α$^+$ ($26.7 \pm 1.6$ vs $40.6 \pm 6.2$, $P = .015$) in Tg thymi compared with WT (supplemental Figure 1). Interestingly, the total number of thymocytes in young *Foxn1*Tg is not higher than that found in young WT, indicating that overexpression of *Foxn1* alters neither the function nor the number of thymopoietic supporting thymic stromal niches. In the context that the thymic size and total thymocyte number are dictated by cortical niches occupied by the double-negative cells as suggested previously,[25] we would speculate that high expression of *Foxn1* does not affect the double-negative cell niches, at least in the young mice.

Although overexpression of *Foxn1* does not affect thymopoiesis in young mice, it does have significant effects on thymopoiesis in

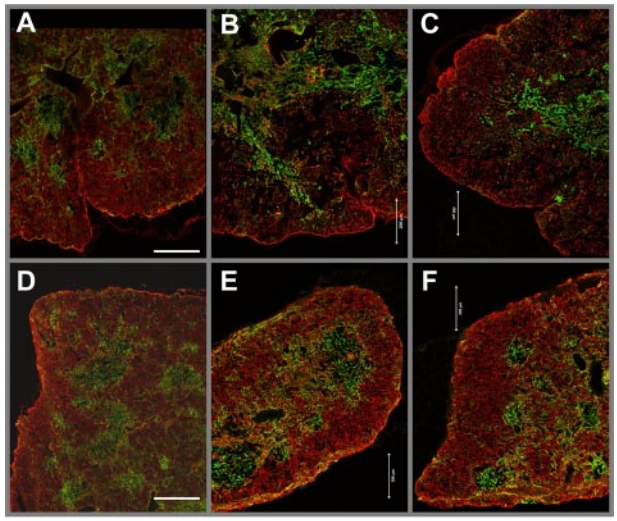


**Figure 6. Double-staining of cortical keratin 8 (red) and medullary keratin 5 (green) in the thymus of WT and *Foxn1*Tg mice (line 60).** Acetone-fixed frozen sections of thymi from 2-month-old (A) and 26-month-old (B-C) WT mice and 2-month-old (D) and 31-month-old (E-F) Tg mice were stained with a rabbit-anti–mouse keratin 5 (green) and rat-anti–mouse keratin 8 (red). Sections were analyzed with a Zeiss LSM 510 confocal microscope. Images were obtained with CApo 40×/1.2 W with a 2 × 2 matrix and digitally stitched using the LSM 510 software. Scale bar represents 200 μm.

**Table 3. Changes in the EpCAM$^+$ MHC II$^+$ and EpCAM$^+$ MHC II$^{hi}$ TEC with age**

| | EpCAM$^+$ MHC II$^+$ TEC cell number | | EpCAM$^+$ MHC II$^{hi}$ TEC | | | |
|---|---|---|---|---|---|---|
| | | | Total cell number | | % Ki-67 positive | |
| Mouse strain | 3 mo | 18-20 mo | 3 mo | 18-20 mo | 3 mo | 18-20 mo |
| WT | 27 481 (11 622) | 7400 (1871)† | 4996 (902) | 554 (175)¶ | 53.1 (21) | 15.1 (5.4)†† |
| *Foxn1*Tg | 68 149 (18 842)* | 15 189 (4159)‡,§ | 25 600 (4860)‖ | 1044 (297)#,** | 56.7 (7.3) | 29.4 (12.5)‡‡,§§ |

The numbers of EpCAM$^+$ MHC II$^+$ and MHC II$^{hi}$ TEC cells were calculated based on the total cell number in the CD45$^-$ compartment and the percentages of EpCAM$^+$ cells within the MHC II$^+$ and MHC II$^{hi}$ subsets as determined by flow cytometry. Data represent mean (SD) values calculated from 5 young (3-month-old) WT, *Foxn1*Tg, old (18-22 months) *Foxn1* Tg mice, and 4 old WT mice. Statistical significance was determined by *t* test: *$P = .003$, vs young WT; †$P = .012$, vs young WT; ‡$P = .016$, vs young *Foxn1* Tg; §$P = .023$, vs old WT; ‖$P < .001$, vs young WT; ¶$P < .001$, vs young WT; #$P = .016$, vs young *Foxn1* Tg; **$P = .040$, vs old WT; ††$P < .001$, vs young WT; ‡‡$P = .002$, vs young *Foxn1* Tg; and §§$P = .017$, vs old WT.

aged thymus. Using the number of copies of germline TCR-Dβ1 and TCR-Dβ2 as an indicator of maturation at the triple-negative stage III, in which TCR-β loci are undergoing rearrangement, we demonstrated that, in old (12-15 months) *Foxn1*Tg thymus, there were 1.7-fold fewer number of germline Dβ1 and Dβ2 copies compared with WT mice. This suggests that more triple-negative stage III cells are undergoing TCRV-β rearrangement or that TN in Tg thymi are more effective in this process; consequently, the total number of sjTREC, a measurement of TCRVα rearrangement, is also higher (3-fold) in the thymus of *Foxn1*Tg. Overall, there was a precipitous decline in thymopoiesis from 2 months to 16 to 19 months in WT compared with *Foxn1*Tg. In *Foxn1*Tg, a similar pattern of decline was only observed much later when the mice were 20 to 26 months old. We also determined that the total number of thymocytes in *Foxn1*Tg at 29 to 32 months is not significantly different from that found in the 20- to 26-month age group. Similarly, the number of thymocytes is not significantly different between the 16- to 19-month and 20- to 26-month age groups. Taken together, we suggest that the decline in thymocyte numbers is attenuated with age in *Foxn1*Tg mice by approximately 6 to 8 months. Thus, although overexpression of Foxn1 does not completely rescue thymic involution and restore thymopoiesis, high expression of Foxn1 does circumscribe the detrimental effect of age on thymopoiesis.

It was suggested that the decline in the frequencies, number, and function of the ETP are partly responsible for thymic involution.[12] Although we also detected a reduction in the frequencies and number of ETP in old WT mice, the frequencies of ETP in old *Foxn1*Tg mice were not reduced and the total number of ETPs in old *Foxn1*Tg was higher than old WT. We noted that the frequencies and total number of ETPs in young WT and *Foxn1*Tg mice were not significantly different. The data indicate that thymic microenvironment with high expression of *Foxn1* does not affect the homing and function of the young ETP, reflecting similar total number of thymocytes in both young WT and *Foxn1*Tg; rather, high expression of *Foxn1* in old mice prevents the decline in the frequency of ETP and lessens the decline in ETP number. Thus, we speculate that high expression of *Foxn1* only partially rescues the intrinsic defect in aged ETP. It has been suggested that Notch signal is required for the generation of ETP from the bone marrow multipotent progenitors.[26] Whether ETP displays a decline in Notch signal with age remains to be determined. However, it is less likely that high expression of *Foxn1* directly affects Notch signal in the aged ETP for 2 reasons. First, expression of the Notch ligand Delta-like 1 (Dl1) and Delta-like 4 (Dl4) is not dependent on the expression of *Foxn1* in the postnatal thymus.[27,28] Second, although we found the expression of both *Dl1* and *Dl4* are reduced in the aged thymus, their reduced expression levels are not restored in thymic stromal of *Foxn1*Tg mice (data not shown).

Age-associated thymic involution is associated with infiltration of fibroblastic and adipose tissue as a result of epithelial-mesenchymal transition.[13] Although thymi from old *Foxn1*Tg are reduced in size compared with young, we observed that there was little infiltration of adipose tissue and the cortical-medullary demarcation remains intact. In the caloric-restricted mice, increases in fibroblasts in the aged thymus are blocked by inhibition of epithelial-mesenchymal transition and adipogenesis through inhibition of peroxisome proliferator-activated receptor-γ expression.[29] A direct role of Foxn1 in adipogenesis remains to be determined.

Previous work has shown that induced-deletion of *Foxn1* causes rapid thymic atrophy mainly because of severe deterioration of mTECs, indicating that Foxn1 expression is critical for the maintenance of mTECs in the postnatal thymus.[9] It was also noted that the MHC II$^{hi}$ mTEC displays high proliferative rate, is responsible for generating the mTEC pool, and is sensitive to reduced expression of *Foxn1*.[10,14,30] Our data showing higher number of EpCAM$^+$ MHC II $^+$ and MHC II$^{hi}$ TECs in *Foxn1*Tg are in agreement with the previous findings.[9,10,14,30] The elevated number of these EpCAM$^+$ mTECs and higher proliferation rate of the EpCAM$^+$ MHC II$^{hi}$ in old *Foxn1* Tg than in WT suggests that the presence of increased number of these cells is responsible for limiting alterations in thymic architecture and attenuate the decline in thymopoiesis with age.

The decline in the production of naive T cells from the thymus caused by age-associated thymic involution results in constriction of the TCR repertoire diversity and expansion of peripheral memory compartments by homeostatic expansion.[2,31] Therefore, the ability to prevent the

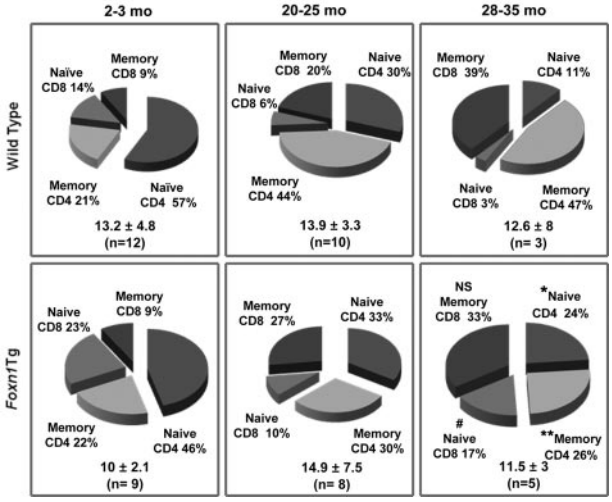


**Figure 7. Changes in the peripheral splenic naive and memory T-cell compartments with age.** Pie charts show the distributions of naive and memory CD4$^+$ and CD8$^+$ T cells in WT and *Foxn1*Tg mice (lines 5 and 60) of 3 different age groups. The percentages of naive and memory cells were calculated based on the average total number of CD3$^+$ CD44$^+$ T cells per spleen (bottom right in each panel, in millions). Values in parentheses indicate the number of animals in each age group. *P* values from *t* test comparing WT and *Foxn1* within an age group: *$P = 0.038$; **$P = 0.019$; #$P = 0.058$. NS indicates not significant.

decline in thymic production of naive T cells and consequently attenuate age-associated expansion of peripheral memory compartments is essential in restoring a young-like peripheral T-cell composition. In our *Foxn1*Tg mice, preventing alterations in thymic architecture with age correlated with improved thymopoiesis, reflected by the higher frequencies of ETP and absolute number of thymocytes. Furthermore, alterations in the proportions of peripheral naive and memory compartments with age were also prevented in aged *Foxn1*Tg mice. Whether the combinatorial effect of preventing age-associated changes in thymopoiesis and peripheral T cells also will lead to improvement of immune response in the old *Foxn1*Tg mice is not known and is currently under investigation.

## Acknowledgments

The authors thank Pat Simms for her excellent technical skill in cell sorting, Mary Kay Olsen for her work on the histology study, Theodore Daniel Logan and Dr Avinash Bhandoola (University of Pennsylvania) for kindly sharing their unpublished thymic epithelial cell isolation protocol, Dr Elaine Fuchs for the keratin 14 construct, and Dr Al Singer (National Cancer Institute) for his valuable advices and support in the early phase of the work.

This work was supported by the National Institutes of Health (R01 AG32809, P.T.L.; R01 AG013874, P.L.W.; T32 AI007508, E.C.Z.; T32 AG031780, E.C.Z.) and Loyola University Stritch School of Medicine (intramural pilot project grant, P.T.L.).

## Authorship

Contribution: E.C.Z. and P.T.L. designed experiments and wrote the paper; P.L.W. contributed to experimental design; E.C.Z., P.A.K., and S.Z. performed research and analyzed data; and N.J.Z.-L. and A.B.F. assisted with construction of the transgenic mice.

Conflict-of-interest disclosure: The authors declare no competing financial interests.

Correspondence: Phong T. Le, Department of Microbiology and Immunology, 2160 S First Ave, Bldg 120, Rm 5644, Maywood, IL 60154; e-mail: ple@lumc.edu.

## References

1. Haynes BF, Markert ML, Sempowski GD, Patel DD, Hale LP. The role of the thymus in immune reconstitution in aging, bone marrow transplantation, and HIV-1 infection. *Annu Rev Immunol.* 2000;18:529-560.
2. Swain S, Clise-Dwyer K, Haynes L. Homeostasis and the age-associated defect of CD4 T cells. *Semin Immunol.* 2005;17(5):370-377.
3. Ortman CL, Dittmar KA, Witte PL, Le PT. Molecular characterization of the mouse involuted thymus: aberrations in expression of transcription regulators in thymocyte and epithelial compartments. *Int Immunol.* 2002;14(7):813-822.
4. Anderson G, Harman BC, Hare KJ, Jenkinson EJ. Microenvironmental regulation of T cell development in the thymus. *Semin Immunol.* 2000;12(5):457-464.
5. Adriani M, Martinez-Mir A, Fusco F, et al. Ancestral founder mutation of the nude (FOXN1) gene in congenital severe combined immunodeficiency associated with alopecia in southern Italy population. *Ann Hum Genet.* 2004;68(3):265-268.
6. Nehls M, Pfeifer D, Schorpp M, Hedrich H, Boehm T. New member of the winged-helix protein family disrupted in mouse and rat nude mutations. *Nature.* 1994;372(6501):103-107.
7. Su DM, Navarre S, Oh WJ, Condie BG, Manley NR. A domain of Foxn1 required for crosstalk-dependent thymic epithelial cell differentiation. *Nat Immunol.* 2003;4(11):1128-1135.
8. Sun L, Guo J, Brown R, Amagai T, Zhao Y, Su DM. Declining expression of a single epithelial cell-autonomous gene accelerates age-related thymic involution. *Aging Cell.* 2010;9(3):347-357.
9. Cheng L, Guo J, Sun L, et al. Postnatal tissue-specific disruption of transcription factor FoxN1 triggers acute thymic atrophy. *J Biol Chem.* 2010;285(8):5836-5847.
10. Chen L, Xiao S, Manley NR. Foxn1 is required to maintain the postnatal thymic microenvironment in a dosage-sensitive manner. *Blood.* 2009;113(3):567-574.
11. Corbeaux T, Hess I, Swann JB, Kanzler B, Haas-Assenbaum A, Boehm T. Thymopoiesis in mice depends on a Foxn1-positive thymic epithelial cell lineage. *Proc Natl Acad Sci U S A.* 2010;107(38):16613-16618.
12. Min H, Montecino-Rodriguez E, Dorshkind K. Reduction in the developmental potential of intrathymic T cell progenitors with age. *J Immunol.* 2004;173(1):245-250.
13. Kvell K, Varecza Z, Bartis D, et al. Wnt4 and LAP2alpha as pacemakers of thymic epithelial senescence. *PLoS One.* 2010;5(5):e10701.
14. Gray DH, Seach N, Ueno T, et al. Developmental kinetics, turnover, and stimulatory capacity of thymic epithelial cells. *Blood.* 2006;108(12):3777-3785.
15. Vassar R, Rosenberg M, Ross S, Tyner A, Fuchs E. Tissue-specific and differentiation-specific expression of a human K14 keratin gene in transgenic mice. *Proc Natl Acad Sci U S A.* 1989;86(5):1563-1567.
16. Bleul CC, Corbeaux T, Reuter A, Fisch P, Monting JS, Boehm T. Formation of a functional thymus initiated by a postnatal epithelial progenitor cell. *Nature.* 2006;441(7096):992-996.
17. Anderson KL, Moore NC, McLoughlin DE, Jenkinson EJ, Owen JJ. Studies on thymic epithelial cells in vitro. *Dev Comp Immunol.* 1998;22(3):367-377.
18. Rodewald HR. Thymus organogenesis. *Annu Rev Immunol.* 2008;26:355-388.
19. Balciunaite G, Keller MP, Balciunaite E, et al. Wnt glycoproteins regulate the expression of FoxN1, the gene defective in nude mice. *Nat Immunol.* 2002;3(11):1102-1108.
20. Cai J, Lee J, Kopan R, Ma L. Genetic interplays between Msx2 and Foxn1 are required for Notch1 expression and hair shaft differentiation. *Dev Biol.* 2009;326(2):420-430.
21. Patel SR, Gordon J, Mahbub F, Blackburn CC, Manley NR. Bmp4 and noggin expression during early thymus and parathyroid organogenesis. *Gene Expr Patterns.* 2006;6(8):794-799.
22. Terszowski G, Muller SM, Bleul CC, et al. Evidence for a functional second thymus in mice. *Science.* 2006;312(5771):284-287.
23. Klug DB, Carter C, Gimenez-Conti IB, Richie ER. Cutting edge: thymocyte-independent and thymocyte-dependent phases of epithelial patterning in the fetal thymus. *J Immunol.* 2002;169(6):2842-2845.
24. Klug DB, Carter C, Crouch E, Roop D, Conti CJ, Richie ER. Interdependence of cortical thymic epithelial cell differentiation and T-lineage commitment. *Proc Natl Acad Sci U S A.* 1998;95(20):11822-11827.
25. Prockop SE, Petrie HT. Regulation of thymus size by competition for stromal niches among early T cell progenitors. *J Immunol.* 2004;173(3):1604-1611.
26. Sambandam A, Maillard I, Zediak VP, et al. Notch signaling controls the generation and differentiation of early T lineage progenitors. *Nat Immunol.* 2005;6(7):663-670.
27. Itoi M, Tsukamoto N, Amagai T. Expression of Dll4 and CCL25 in Foxn1-negative epithelial cells in the post-natal thymus. *Int Immunol.* 2007;19(2):127-132.
28. Tsukamoto N, Itoi M, Nishikawa M, Amagai T. Lack of delta like 1 and 4 expressions in nude thymus anlages. *Cell Immunol.* 2005;234(2):77-80.
29. Yang H, Youm YH, Dixit VD. Inhibition of thymic adipogenesis by caloric restriction is coupled with reduction in age-related thymic involution. *J Immunol.* 2009;183(5):3040-3052.
30. Gillard GO, Farr AG. Features of medullary thymic epithelium implicate postnatal development in maintaining epithelial heterogeneity and tissue-restricted antigen expression. *J Immunol.* 2006;176(10):5815-5824.
31. Sprent J, Cho JH, Boyman O, Surh CD. T cell homeostasis. *Immunol Cell Biol.* 2008;86(4):312-319.